Composites: Part A 200 (2026) 109347

Contents lists available at ScienceDirect

Composites Part A

journal homepage: www.elsevier.com/locate/compositesa

Short communication

Effect of loading rate, viscosity, and binder activation on the bending response of an infiltrated UD-NCF

Renan Miranda Portela [a], Bastian Schäfer [b], Luise Kärger [b], Alfredo Rocha de Faria [c], John Montesano [a,*]

[a] Composites Research Group, Department of Mechanical & Mechatronics Engineering, University of Waterloo, 200 University Ave. West, Waterloo, ON N2L 3G1, Canada
[b] Karlsruhe Institute of Technology (KIT), Institute of Vehicle System Technology (FAST), Karlsruhe, Germany
[c] Department of Mechanical Engineering, Instituto Tecnológico de Aeronáutica (ITA), Praça Marechal Eduardo Gomes, 50, São José dos Campos, SP 12228-900, Brazil

ARTICLE INFO

Keywords:
Wet compression molding
Forming
Infiltrated bending tests
Binder-stabilized unidirectional non-crimp fabric

ABSTRACT

Assessing the bending response of infiltrated reinforcement fabrics is crucial in wet compression molding (WCM) as it affects macroscopic wrinkling. Binder-stabilized fabrics may be used in WCM to improve handleability and reduce defects, necessitating their characterization. This study examines the bending behavior of an infiltrated binder-stabilized carbon fiber unidirectional non-crimp fabric (UD-NCF), focusing on the effects of viscosity, loading rate, and binder pre-activation. Infiltration reduces bending stiffness compared to dry fabric owing to lubrication and lower tow-stitch friction, while higher loading rates increase bending stiffness for all considered conditions. Moreover, binder pre-activation increases fabric stiffness by enhancing tow-stitch cohesion and friction. As the first investigation on infiltrated binder-stabilized UD-NCF bending, this work advances understanding of the complex bending response.

1. Introduction

Liquid composite molding (LCM) processes have been used for over 50 years [1] to manufacture fiber-reinforced plastic composite parts with complex shapes and high fiber volume fractions. LCM processes have the potential for high production volumes at relatively low manufacturing cost, which may compensate for high raw material costs [1–5]. This class of manufacturing processes includes Resin Transfer Molding (RTM), High Pressure-RTM (HP-RTM), and Wet Compression Molding (WCM). Among these processes, WCM using highly reactive resins is particularly promising for mass production. Unlike RTM processes, WCM does not require a fabric preforming step or use of sophisticated metering equipment to inject resin into the mold or use of a large press, which may increase processing throughput and decrease the cost of the final fabricated part [4,6,7]. A typical WCM process consists of five steps, as illustrated in Fig. 1. The fabric layers are first cut and stacked before being introduced into the preheated mold. Next, the resin is dispensed onto the fabric stack before the mold is closed. In automated setups, resin application may be conducted outside of the mold, and the impregnated fabric stack introduced into the mold. Thereafter, forming and infiltration of the fabric occur simultaneously during the molding phase, removing the need for a dedicated fabric preforming step. Finally, the resin cures, and the final part is removed from the mold.

Among the fabrics used in WCM processes, continuous reinforcements such as woven and unidirectional non-crimp fabrics (UD-NCF) are commonly employed. UD-NCFs have recently gained attention in the automotive industry owing to their excellent drapability, which is well-suited for LCM processes [8]. UD-NCFs consist of parallel-oriented fiber tows held together by stitching threads, which ensure the structural integrity of the reinforcement and provide stability during handling and manufacturing [8–11]. Unlike woven fabrics that comprise varying degrees of interlacing, the aligned fiber tows in UD-NCFs are not interlaced, which enhances the in-plane mechanical properties of the fabricated composite material. According to Rudd et al. [12], NCF composites can achieve up to 15 % greater load-bearing efficiency compared to similar woven fabrics, offering a higher potential for lightweight structures.

For structural components, many layers of UD-NCF oriented along different directions are required to meet desired anisotropic properties and performance requirements, which could result in thick components.

* Corresponding author.
E-mail address: john.montesano@uwaterloo.ca (J. Montesano).

https://doi.org/10.1016/j.compositesa.2025.109347
Received 8 August 2025; Received in revised form 21 September 2025; Accepted 5 October 2025
Available online 6 October 2025

For relatively large components comprising multidirectional layers, this would require the application of a significant quantity of resin to the flat fabric stack (i.e., step 3 in Fig. 1). However, producing such components using WCM processes—especially in molds with deep cavities—presents challenges related to resin management since the UD-NCF stack may drape under gravity due to the mass of the applied resin. Draping of the fabric stack prior to closing the mold may lead to resin pooling and fabric shifting within the mold, which could lead to defects such as dry spots, voids, and severe fabric wrinkling. A promising solution to address this issue is the use of binder-stabilized UD-NCF, where pre-activation of the binder before insertion of the flat stack into the mold may provide increased fabric bending stiffness [13] and enable improved resin management. Stabilizing binders are either thermoplastic or uncatalyzed epoxy resins, available in either solvent-based liquid or dry powder form [14–16]. Stabilizing binders are typically used to keep fabric layers adhered to one another and maintain fabric integrity during operations such as trimming and handling [14]. At the same time, stabilizing binders are necessary for preforming of UD-NCF stacks during RTM processes. However, the use of binder-stabilized fabrics may also introduce challenges, as they can affect processing conditions and fabric formability.

Most studies focused on characterizing binder-stabilized fabrics investigated the influence of the stabilizing binder on fabric permeability and resin viscosity. Estrada et al. [14] reported that increasing the binder concentration leads to reduced fabric permeability. Brody and Gillespie [15] examined the effects of thermoplastic binder on vinyl ester resin and found that the binder powder gradually dissolved in the resin, decreasing in particle size over time. Additionally, they observed a significant delay in resin curing and an increase in viscosity. Yoo et al. [16] investigated the influence of epoxy binder on the permeability and friction coefficients of woven fabric, revealing that the stabilizing binder can reduce permeability by up to 98 % and increase the fabric friction coefficient by as much as 200 %. Neunkirchen et al. [17] reported that the molten stabilizing binder forms an interlayer film, which blocks some capillary channels and slows down capillary flow.

Several studies have concentrated on evaluating the impact of stabilizing binders on intra-ply draping mechanisms, including membrane and compaction behaviors (see Fig. 2). Wei et al. [18] examined the compaction behavior of woven fabrics and NCFs, noting that the application of stabilizing binder increases the initial thickness and relaxation of the stack. However, it also reduces the elastic recovery, enhancing the viscoelastic properties of the fabric stack. Portela et al. [19] analyzed the effect of pre-activating the stabilizing binder on the membrane performance of both dry and impregnated UD-NCF. Their findings indicate that the molten binder coats the fiber tows, increasing cohesion between the tows and stitching yarns, which in turn enhances membrane stiffness. Broberg et al. [20] investigated the transverse shear behavior of a binder-stabilized glass UD-NCF to better comprehend the forming process in the manufacture of wind turbine blades. Their results demonstrated an increase in load corresponding with an increase in deformation rate.

Given the critical importance of draping mechanisms within the WCM process and the objective of optimizing the final components, it is essential to thoroughly characterize the fabric utilized in manufacturing [22]. In previous studies, the bending mechanism was frequently neglected due to the low stiffness characteristic of fabrics, with primary focus on membrane behavior [23,24]. However, flexural behavior plays a key role in describing fiber curvature and can significantly influence the wrinkle formation during the forming stage, compromising the mechanical performance of the final part [25–29]. Senner et al. [30] emphasized that low bending stiffness can lead to substantial fabric deformation under minimal bending loads.

Several test methods have been developed to characterize the bending behavior of engineering textiles, including variations of the cantilever test (e.g., Peirce, vertical, and free-hanging tests), rheometer bending test (RBT), and buckling tests [31]. Traditional three- and four-point bending tests are, in general, not employed for fabric characterization due to their low flexural stiffness caused by relative slippage between fiber tows. These test setups are typically reserved for thick reinforcements or small composite samples with higher bending stiffness and are therefore avoided in fabric studies [23,26,32]. Krogh et al. [31] compared various testing methods for characterizing fabric bending stiffness. The first method, known as the Peirce cantilever test [33], involves a simple setup with an inclined plane over which a fabric strip overhangs. Bending stiffness is estimated when the tip of the fabric contacts the plane, assuming a constant stiffness. However, this assumption may oversimplify fabric behavior and fail to capture nonlinear responses [31]. Despite its limitations, the simplicity of the Peirce method has contributed to its popularity among researchers [23,31,34–37]. Poppe et al. [32] observed that some Peirce method variations use a weight to clamp the non-overhanging end of the fabric strip. This weight compresses the fabric under an undetermined degree of compaction, altering boundary conditions and potentially introducing inconsistencies in the results. Alternatively, the Kawabata bending test (KES-FB2) employs a specialized device with two clamps securing the specimen, while one clamp rotates to impose a controlled curvature and loading rate. This method enables direct measurement of moment–curvature curves, even under cyclic loading conditions, and effectively captures nonlinear, hysteretic, and loading-rate-dependent behaviors. An adaptation of this setup was introduced by Sachs and Akkerman [28], which modifies the test for compatibility with rheometer equipment—referred to as the Rheometer Bending Test (RBT). The RBT is widely recommended in the literature for its accuracy and capability to characterize rate-dependent, temperature-sensitive, and hysteretic responses of fabrics [31,32].

Recent studies in the literature have focused on the bending behavior of binder-stabilized fabrics. Broberg et al. [38] investigated the forming of binder-stabilized glass fiber NCF for manufacturing thick parts and found that, in transition regions, the stabilizing binder may increase wrinkle formation. They also observed that large compressive loads can cause the formation of large wrinkles and damage to the binder material. In a subsequent study, Broberg et al. [39] characterized the nonlinear behavior of glass fiber NCF using a modified cantilever test. They concluded that incorporating material nonlinearities in the simulation model improves the prediction of wrinkle formation. Similarly, Ghazimoradi et al. [40] used the modified cantilever method to characterize the nonlinear bending behavior of a dry and inactivated binder-stabilized carbon fiber UD-NCF. They reported significant anisotropy,

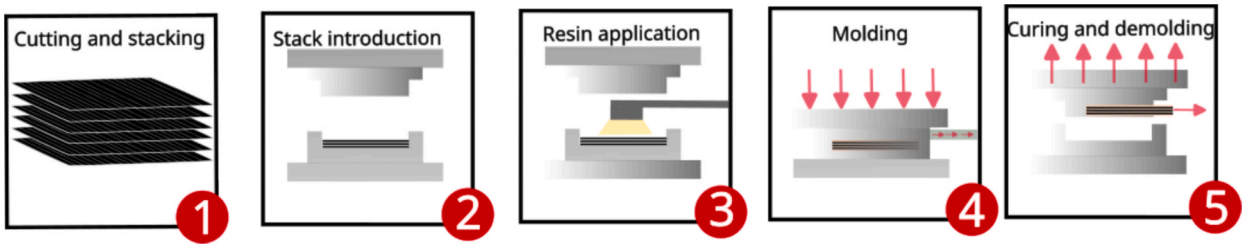

Fig. 1. Schematic of the steps for a typical WCM process.

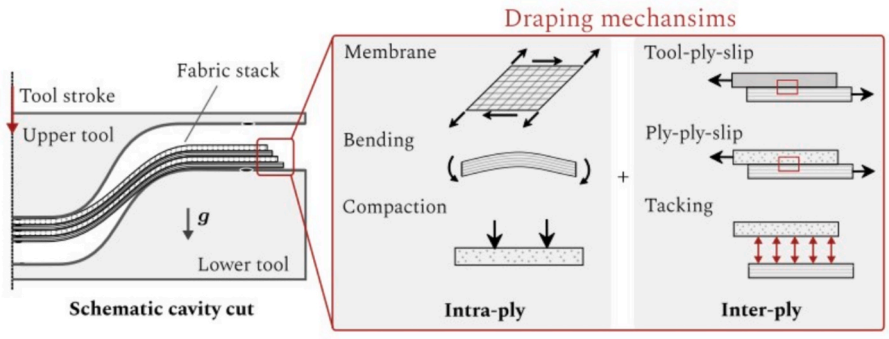

Fig. 2. Draping mechanism present during the WCM process [21].

with low bending stiffness in the direction transverse to the fiber tows and notable stiffness along the fiber direction. The characterization data were later used to calibrate an anisotropic material model implemented in commercial finite element software [41]. Broberg et al. [39] and Ghazimoradi et al. [40] investigated the behavior of a binder-stabilized UD-NCF; however, neither considered the effect of binder pre-activation nor the impregnation of the fabric, due to the targeted manufacturing processes.

Despite advancements in understanding the bending behavior of binder-stabilized UD-NCFs, it is important to note that in the WCM process, forming occurs during the molding phase (Fig. 1) when the fabric is impregnated. Therefore, all draping mechanisms, including bending behavior (Fig. 2), may behave differently from those reported in previous studies [38,40], which did not consider fabric infiltration or pre-activation of the binder due to the different manufacturing processes that were investigated. One study that did consider the influence of infiltrated fluid viscosity on the bending response of reinforcement fabrics was conducted by Poppe et al. [32]. An RBT test and a variation of the Peirce test were used to characterize the bending behavior of an infiltrated woven fabric. Although Pope et al. [32] were the first to study the bending response of an impregnated reinforcement fabric, their study exclusively considered a non-binder-stabilized woven fabric. This left a gap in the literature for other binder-stabilized fabrics, particularly UD-NCFs, which may influence the fabric's behavior. To date, no studies have focused on characterizing the bending response of infiltrated binder-stabilized UD-NCFs and the corresponding influence of binder pre-activation. In this study, the bending behavior of an impregnated binder-stabilized carbon fiber UD-NCF is investigated through a series of RBTs. Consequently, the influence of the loading rate, fluid viscosity, and activation of binder on the bending response is investigated.

2. Fabric material and experimental methodology

2.1. Fabric description and specimen preparation

The studied binder stabilized UD-NCF, namely PX35-UD300 (Zoltek, US), comprised axially oriented parallel tows, each composed of 50 K continuous PX35 carbon fibers (CF). The tows were stitched together with a 76 dtex polyester yarn in a tricot pattern. In addition, the textile included transversely oriented supporting glass fibers (GF) with low linear density to improve handleability, while a thermosetting polymer powder binder was dispersed on the stitch tricot pattern surface (Fig. 3). The textile has a total areal density of 333 g/m^2. Fabric specimens with dimensions 140 mm × 60 mm (with CF aligned along the longer dimension) were cut from a roll using an automated cutting table (Zünd Systemtechnik AG, Switzerland). Lastly, 20 cSt and 100 cSt silicone oils were used to impregnate a subset of the specimens, as they represent the viscosities of various epoxy resins under elevated temperature processing conditions.

2.2. Rheometer bending test setup

Fig. 4 illustrates the test setup used for the RBTs, comprising a customized MCR501 rheometer (Anton Paar, Austria), an oil collector plate, and an enlarged frame utilized for supporting and bending the fabric specimen over the angular range from 0 to 60°. The use of an enlarged frame enhanced the reproducibility of the tests. This frame is subdivided into two fixtures: a fixed fixture that supports the rectangular fabric specimen on one side and a rotating fixture that supports the specimen on the opposite side. Teflon tape was applied to the frame fixtures to mitigate friction with the fabric specimen. Additionally, industrial duct tape was fixed on both ends of each specimen to maintain the CF tow orientation along the horizontal direction. For the infiltrated

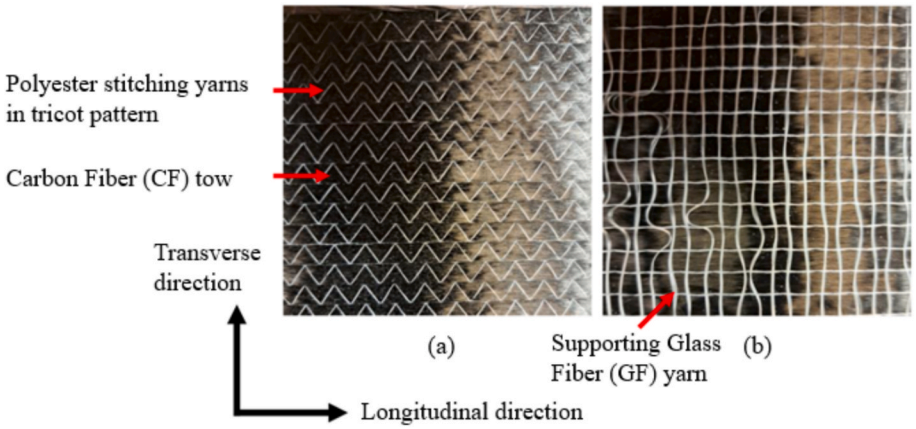

Fig. 3. Images of the PX35-UD300 UD-NCF showing different constituents and microstructure: (a) stitch tricot pattern surface, and (b) supporting glass fiber surface.

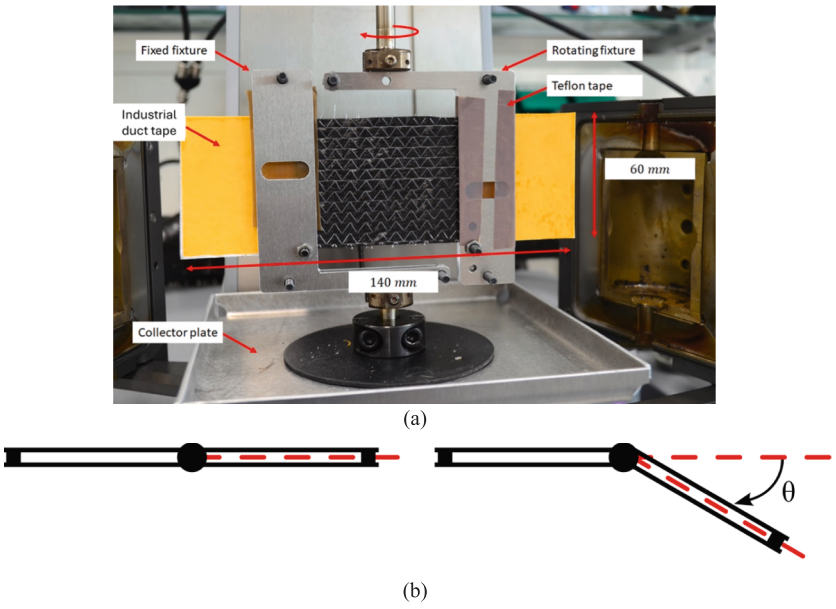

Fig. 4. (a) Setup of the RBT with a fabric specimen mounted in the frame fixtures, including a prepared specimen and its measurements, (b) top-view schematic of the RBT setup.

samples, 2 ml of silicon oil was dispensed with a syringe onto the central region (approximately 70 mm × 60 mm), where the bending occurs, to avoid wetting the contact interfaces. Following impregnation, the specimens rested for 2 min prior to testing to ensure complete saturation.

Bending tests were performed at room temperature under four distinct conditions (refer to Table 1). While typical WCM processes are performed at elevated temperatures in a pre-heated mold, the fabric is usually formed before reaching the mold temperature. Consequently, tests at elevated temperatures were not considered herein as they are not representative of WCM processes. For the first three conditions, specimens had their binder system pre-activated at 120 °C for 20 min prior to being supported in the fixtures. These specimens were subjected to an applied angular velocity of either 0.1, 1.0, or 10.0 RPM. The binder present in the investigated fabric is a thermosetting polymer, which, when thermally activated, melts and coats the fabric. Following pre-activation, subsequent variations in temperature would have a low influence on the binder, given that this process is irreversible; however, this factor was not considered in the study. For the fourth condition, specimens with no binder pre-activation were utilized, and an angular velocity of 1.0 RPM was applied. For all conditions, three viscosity cases were considered: dry, silicone oil with a viscosity of 20 cSt, and silicone oil with a viscosity of 100 cSt, yielding a total of 12 test cases. Both oil viscosities mimic the viscosity of typical resins during the manufacturing process. Note, a total of 8 repeated tests were performed for all test cases (i.e., 96 tests in total).

Table 1
Different conditions tested using the RBT setup.

Condition	Binder state	Angular velocity [RPM]	Viscosity [cSt]	Number of specimens
1	Activated	0.1	Dry	8
			20	8
			100	8
2	Activated	1	Dry	8
			20	8
			100	8
3	Activated	10	Dry	8
			20	8
			100	8
4	Inactivated	1	Dry	8
			20	8
			100	8

The rheometer was set to move from 0° to 60° for every test, considering the different bending rates. Data acquisition was performed at intervals of 0.5 s, 0.05 s, and 0.01 s for the tests at 0.1, 1.0, and 10.0 RPM, respectively. The bending moment, $M(\theta)$, and rotation angle, θ, were recorded for each experimental test. For every condition, the rotation angle was converted to curvature κ using [31,32]:

$$\kappa = \frac{\tan\left(\frac{\theta_i^{Rheo}(t)}{2}\right)}{R}, \tag{1}$$

where R is the rheometer bending radius, assumed to be constant throughout the test. Next, the moment $M(\kappa)$ was divided by the sample width. The width-normalized bending stiffness (i.e., bending stiffness per unit width) was defined as the slope of the width-normalized moment–curvature plot.

To verify the statistical significance of the influence of loading rate, impregnation fluid viscosity, and binder pre-activation on the fabric bending stiffness, pairwise analyses were conducted on width-normalized bending stiffness for two conditions using a two-sample T-test. The null hypothesis for a T-test assumes no difference between the sample data and is accepted when the corresponding p-value is greater than 0.05. Otherwise, the null hypothesis is rejected, indicating a statistically significant difference.

3. Results and discussion

To ensure consistent analysis of all collected data for each condition (Table 1), the moment values were interpolated within the range from 0° to 60° to align the angle measurements across all eight specimens. Then, the angle measurements were converted to curvature, and the moments were normalized. The mean and standard deviation values for the normalized moment were calculated for the set of specimens for each investigated condition, represented by solid lines and shaded regions in Fig. 5, respectively. It is worth noting that, across all conditions, the results were repeatable with minimal scatter, and the normalized moment values exhibited a linear increase with increasing curvature. A small number of specimens exhibited responses that deviated from the

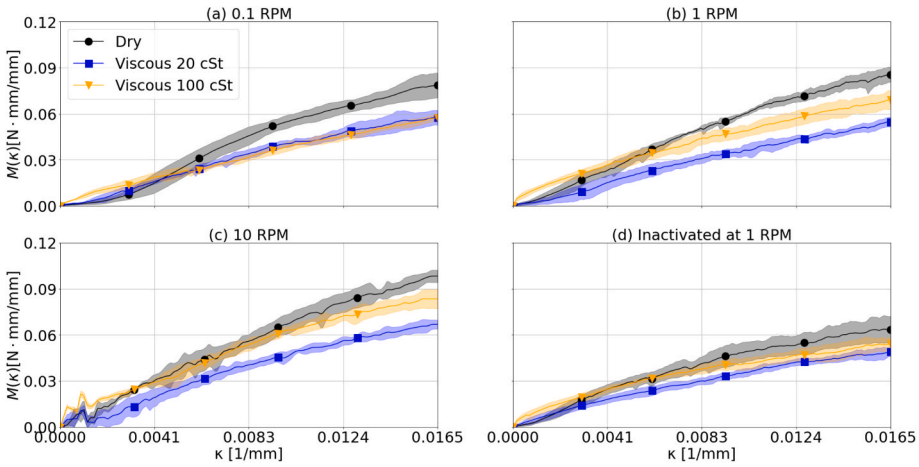

Fig. 5. Normalized moment–curvature plots for the four tested conditions, each including dry, impregnated with 20 cSt silicone oil, and impregnated with 100 cSt silicone oil infiltration cases: (a) Condition (1) – binder pre-activated and 0.1 RPM velocity, (b) Condition 2 – binder pre-activated and 1 RPM velocity, (c) Condition 3 – binder pre-activated and 10 RPM velocity, (d) Condition 4 – binder inactivated and 1 RPM velocity.

majority of repeated tests for each condition. These outliers were omitted from the analysis, as they were not considered to be representative. Additionally, the normalized bending stiffness for each condition was determined as described in the previous section, utilizing the full range of curvature data from 0 to 0.0165 mm^{-1}. Tables 2 and 3 present the normalized bending stiffness values for the activated and inactivated specimens, respectively, while these data are also plotted in Fig. 6.

As mentioned in the previous section, the fabric samples were extracted from the same binder-stabilized fabric roll with a CNC table machine. The relatively minor variability of the bending test results may be attributed to several factors, including material defects, sample preparation, and the testing procedure. Previous studies observed that stitching yarn cross-over points in NCFs can be unevenly distributed, which may lead to in-plane tow misalignment and out-of-plane crimp [42–44]. Uneven stitching yarn patterns may influence the size of the fiber tow and the thickness of the layer. Thus, it is plausible that these variations may lead to some degree of scatter in the bending stiffness, albeit deemed to be minor in this study. In addition, the application of stabilizing binder powder may also vary across different regions of the roll. This variation may lead to higher bending stiffness in specimens with greater binder content. Moreover, although the amount of silicone oil was carefully measured before impregnating each specimen, some minor variations in the amount of oil and impregnation uniformity may have also affected the bending response of the specimen and contributed to scatter in the presented data. Variations could have also been induced during the fabric specimen preparation, particularly during cutting with the CNC table machine. The cutting procedure involved several steps, including aligning the fabric on the cutting table. The fabric may have been slightly misaligned, resulting in slightly off-axis specimens and lower fabric bending responses. Lastly, data scatter may also be attributed to positioning of the fabric specimens during the tests. As the fabric specimens were not clamped to the fixture, they may have exhibited some inclination at the beginning of the tests or minor shifting as the moving frame rotated.

The normalized bending stiffness of the dry UD-NCF along the fiber direction for the condition with inactivated binder at 1 RPM angular velocity (see Table 3) is approximately 64 % greater than the normalized bending stiffness of 2.41 N mm for a dry non-bindered 12 K carbon fiber plain woven fabric studied by Poppe et al. [32], using the same RBT setup. The comparatively lower bending stiffness of this woven fabric is presumably attributable to the presence of yarn interlacing and the smaller tow size, when contrasted with the UD-NCF examined herein. Additionally, the normalized bending stiffness of the dry UD-NCF along the fiber direction for the same condition is approximately 7.34 % greater than the normalized bending stiffness of 3.68 N mm for a binder-stabilized UD glass fabric with a tricot stitching pattern and an areal density of 1322 g/m^2 investigated by Krogh et al. [31] using an RBT setup. This difference can be attributed to several factors, including the lower angular velocity used in Ref. [31] (i.e., 0.75 RPM) and differences in the fabric composition and architecture. Although a one-to-one comparison with a similar fabric is not feasible, these comparisons reveal that the bending stiffness of the studied carbon fiber UD-NCF along the fiber direction is relatively high in comparison to other common reinforcement fabrics. More generally, the findings also highlight a significant influence of loading rate, viscosity, and binder pre-activation on the fabric's bending behavior, which will be discussed hereafter.

The effect of loading rate on the fabric bending stiffness is illustrated qualitatively in Fig. 5 (a), (b), and (c). As the angular velocity increased from 0.1 RPM to 1 RPM and from 1 RPM to 10 RPM for the dry-activated binder case, the average normalized bending stiffness increased by 1.65 % and 13.74 %, respectively (Table 2). This observation aligns with previous studies indicating the dependency of bending stiffness on loading rate for dry woven fabrics [32,45]. The bending stiffness of UD-NCFs is influenced by the interaction between fiber tows and stitching yarns [40]. As the fabric bends, the stitching yarns slide over the fiber tows, generating friction between the fabric constituents. Bending occurs once all the frictional resistance is overcome [46,47]. At higher loading rates, there is less time for the fabric constituents to overcome static friction, resulting in reduced relative sliding and consequently higher measured fabric bending stiffness. Additionally, since the fabric specimens were not clamped to the RBT fixture, some slippage was observed, as reported in Ref. [32], with this effect being more

Table 2
Normalized bending stiffness values of the pre-activated samples (Conditions 1 – 3).

Loading rate [RPM]	Dry [N mm]	Viscosity 20 cSt [N mm]	Viscosity 100 cSt [N mm]
0.1	5.44	3.77	3.35
1	5.53	3.41	3.83
10	6.29	4.49	5.12

Table 3
Normalized bending stiffness values of the inactivated samples (Condition 4).

Loading rate [RPM]	Dry [N mm]	Viscosity 20 cSt [N mm]	Viscosity 100 cSt [N mm]
1	3.95	2.91	2.88

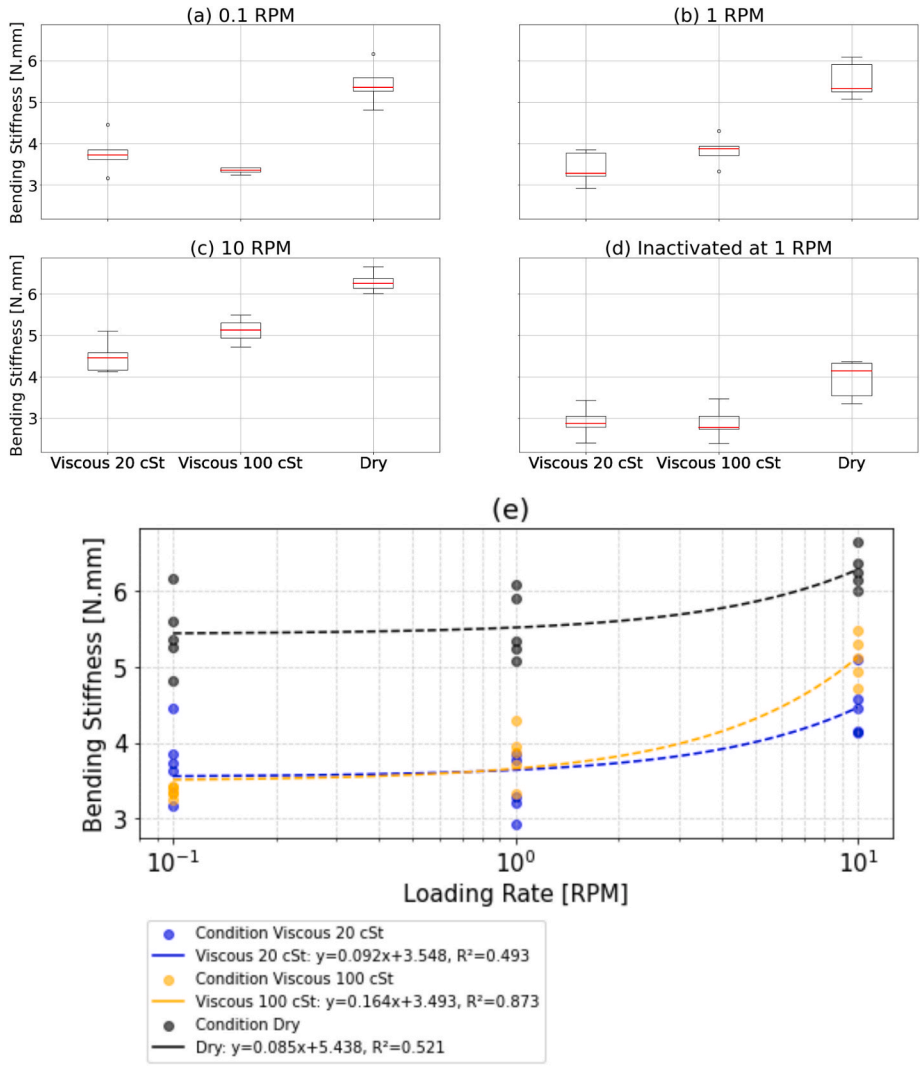

Fig. 6. Normalized bending stiffness for the four tested conditions, each including impregnated with 20 cSt silicone oil, impregnated with 100 cSt silicone oil infiltration, and dry cases: (a) Condition (1) – binder pre-activated and 0.1 rpm velocity, (b) Condition 2 – binder pre-activated and 1 rpm velocity, (c) Condition 3 – binder pre-activated and 10 rpm velocity, and (d) Condition 4 – binder inactivated and 1 rpm velocity. (e) Normalized bending stiffness vs loading rate for the indicated infiltration case.

pronounced at an angular velocity of 0.1 RPM. Consequently, lower loading rates resulted in lower apparent bending stiffness because of the easier overcoming of static friction. Interestingly, the effect of loading rate on the specimens impregnated with a 20 cSt viscosity oil was much less noticeable (Table 2). The impregnation of the fabric with a low-viscosity oil has reduced friction between the fiber tows and stitching and enabled increased relative movement, which has reduced the degree of the influence of loading rate on fabric bending stiffness. Moreover, for the specimens impregnated with a 100 cSt viscosity oil, the normalized bending stiffness increased by 14.32 % and 33.68 % (Table 2) as the angular velocity increased from 0.1 to 1 RPM and from 1 RPM to 10 RPM, respectively (i.e., a similar trend to that of the dry pre-activated binder specimens). However, the stronger influence of loading rate on specimens infiltrated with higher viscosity oil may be because the frictional bending restraint is relatively greater compared to specimens infiltrated with lower viscosity oil. Table 4 lists the p-values associated with each pair of normalized bending stiffness data for each loading rate and impregnation condition. Only two of the nine comparisons yielded p-values greater than 0.05, confirming that an increase in loading rate results in a statistically significant increase in fabric bending stiffness.

The impregnated fabric specimens exhibited lower bending stiffness when compared to dry specimens for each condition, which is shown qualitatively in Fig. 5. For example, the normalized bending stiffness of the dry specimens and specimens impregnated with 100 cSt viscosity oil tested at an angular velocity of 1 RPM (Fig. 5b, Table 2) were, respectively, 62.17 % and 12.32 % greater than that of the specimens impregnated with a 20 cSt viscosity oil. Similar findings were reported in Ref. [32] for a carbon fiber woven fabric, where it was determined that the silicone oil acts as a lubricant, reducing friction among the fiber tows and supporting yarns, which resulted in lower fabric stiffness. Similarly, in this study, the friction between the carbon fiber tows and the polyester stitching yarns was reduced for impregnated specimens, leading to a reduction in the fabric's bending stiffness. The observed

Table 4
P-values obtained through T-Test comparing the normalized bending stiffness for different loading rate pairs, for each impregnation case. Note, green text refers to P-values > 0.05.

	0.1 RPM x 1 RPM	0.1 RPM x 10 RPM	1 RPM x 10 RPM
Dry	7.64×10^{-1}	8.99×10^{-3}	9.79×10^{-3}
Viscous 20	2.29×10^{-1}	2.99×10^{-2}	2.55×10^{-3}
Viscous 100	1.80×10^{-2}	1.50×10^{-6}	2.75×10^{-4}

increase in bending stiffness for the specimens impregnated with the higher viscosity oil may be due to greater friction caused by the 100 cSt oil in comparison to 20 cSt oil [32]. It must be noted that at higher angular velocities (Fig. 5c, Table 2), the bending behavior of the sample impregnated with 100 cSt silicone oil converged with that of the dry fabric samples, possibly due to the comparable frictional resistance between the fabric constituents and, thus, similar bending restriction when compared to the dry samples [47,48]. Another interesting observation is that the bending stiffness of the specimens with inactivated binder (Fig. 5d, Table 3) was notably less influenced by the presence of viscous oil. This finding might be due to the relatively low friction between the fiber tows with inactivated stabilizing binder and the stitching, which led to reduced sensitivity to impregnation oil viscosity on the bending stiffness. Similar two-sample T-tests were performed (Table 5), revealing that for all but two test case comparisons, there were statistically significant differences in the normalized bending stiffness.

Lastly, the effect of binder pre-activation on the bending behavior was evaluated by comparing the results illustrated in Fig. 5(b) and 5(d) as well as Tables 2 and 3. It was observed that binder pre-activation enhances bending stiffness, attributable to the improved cohesion provided by the molten binder [19]. When the fabric is subjected to heat, the binder melts and coats the fiber tows, increasing inter- and intra-tow friction and consequently bending stiffness. This effect was more pronounced in the dry samples, indicating that the impregnation fluid viscosity tends to counteract the influence of the activated binder. Broberg et al. [38] also reported variations in bending stiffness in binder-stabilized non-crimp fabric, which could potentially lead to an increased propensity for wrinkle formation. Once again, two-sample T-tests were conducted, and none of the comparisons failed to reject the null hypothesis (Table 6).

4. Conclusions

This study has shown that the applied angular velocity, pre-activation of the stabilizing binder, and the viscosity of the impregnation fluid significantly influence the bending behavior of a carbon fiber unidirectional non-crimp fabric (UD-NCF), particularly at large curvatures, which are likely to occur in components with complex geometries fabricated via wet compression molding (WCM) process. More specifically, pre-activation of the stabilizing binder and increased loading rate contributed to an increase in bending stiffness across all three infiltrated conditions (i.e., dry, infiltrated with 20 cSt silicone oil, and infiltrated with 100 cSt silicone oil), owing to increased friction between the carbon fiber tows and stitching yarns. However, infiltration of the fabric with a low viscosity fluid resulted in a decrease in bending stiffness relative to the dry condition due to decreased tow-stitch friction. In contrast, the decrease was less pronounced for the higher-viscosity oil infiltration condition considered in this study. The influence of pre-activated stabilizing binder and fabric impregnation observed in this investigation for the studied UD-NCF is expected to be similar for other types of binder-stabilized fabrics, although the magnitude of these effects may vary depending on the specific fabric architectures. It is important to note that for a WCM process, an additional binder pre-activation step will be required prior to dispensing resin on the fabric stack, which would increase process complexity to some extent due to heating requirements. In an industrial setting, the addition of this step would not affect the overall process cycle time, so long as the binder pre-activation time is less than the cure and demolding time.

Table 5
P-values obtained through T-Test comparing the normalized bending stiffness of pre-activated binder specimens for different fabric impregnation case pairs, for each loading rate. Note, green text refers to P-values > 0.05.

	Dry x Viscous 20	Dry x Viscous 100	Viscous 20 x Viscous 100
0.1 RPM	5.83×10^{-4}	1.48×10^{-5}	8.59×10^{-2}
1 RPM	4.17×10^{-5}	1.47×10^{-4}	1.13×10^{-1}
10 RPM	2.45×10^{-5}	1.52×10^{-4}	2.25×10^{-2}

Table 6
P-values obtained through T-Test comparing the normalized bending stiffness of specimens with and without stabilizing binder pre-activation under different impregnation conditions at 1 RPM.

Dry	Viscous 20	Viscous 100
5.63×10^{-4}	4.82×10^{-2}	4.24×10^{-3}

The generated test data fills a critical gap in the literature and can help improve material models for future forming simulations of binder-stabilized UD-NCFs. An improved understanding of the bending behavior of UD-NCFs achieved in this study can also be used for optimizing WCM processes. Optimizing the press closing speed and the resin viscosity may aid in suppressing the formation of macroscopic wrinkles. At the same time, the use of a binder-stabilized fabric will increase stiffness, which could lead to better resin management before mold closing while also influencing fabric formability. As shown, the use of a stabilizing binder notably influences the bending response of the studied UD-NCF, where an increase in bending stiffness may potentially reduce the number of wrinkles during forming at the expense of increasing their size as reported by Boisse et al. [11]. Similar findings were reported in Ref [38], where the authors studied a binder-stabilized glass UD-NCF and observed an increase in wrinkle size due to higher fabric bending stiffness. However, forming of continuous reinforcements on complex-shaped molds induces in-plane shear deformation, which can also contribute to the formation of wrinkles on the fabric depending on the forming process boundary conditions. Haanappel et al. [49] investigated the drapability of two fiber-reinforced thermoplastic materials on a mold with a double-curved surface, highlighting that bending stiffness, as well as intra-ply deformation and friction, significantly influence drapability. Significant wrinkling in the double-curved regions was observed, where the authors noted that the number and size of wrinkles are dependent on the fabric properties. Specifically, it was stated that fabrics with greater bending stiffness were more sensitive to wrinkle formation. Nevertheless, these studies have not identified an optimal range of bending stiffness, as the drapability of an engineering textile is influenced by multiple parameters. Despite the important contributions made through the study herein, the connection between bending stiffness, formability, and associated defect formation remains unclear as it likely depends on additional factors, such as the number of layers, ply orientation, and mold shape. Therefore, establishing such a relationship for the studied binder-stabilized UD-NCF is left for future work. Broadly, this work aims to assess the potential trade-offs between increased fabric stiffness and formability for complex shapes typical of real-world applications.

Additional future work is planned that is worth mentioning. The bending behaviour of the UD-NCF along the transverse direction was not studied herein, given that the fabric bending stiffness along this direction is anticipated to be orders of magnitude lower than that along the longitudinal direction. The resolution of the rheometer would not adequately capture the low-magnitude transverse bending stiffness. Future work will focus on modifying the rheometer bending test setup to enable testing along the transverse direction. Finally, future studies will explore whether binder type, concentration, and form, fiber tow count, and stitching pattern influence the bending stiffness of the UD-NCFs. The rate-dependent bending response of the UD-NCF will also be studied, since related data is important for developing rate-dependent forming models.

CRediT authorship contribution statement

Renan Miranda Portela: Writing – original draft, Validation, Methodology, Investigation, Formal analysis. **Bastian Schäfer:** Writing – review & editing, Methodology, Formal analysis. **Luise Kärger:**

Writing – review & editing, Supervision, Resources, Conceptualization. **Alfredo Rocha de Faria:** Writing – review & editing, Validation, Supervision. **John Montesano:** Writing – review & editing, Validation, Supervision, Resources, Project administration, Funding acquisition, Conceptualization.

Declaration of competing interest

The authors declare that they have no known competing financial interests or personal relationships that could have appeared to influence the work reported in this paper.

Acknowledgements

This study was funded by the Natural Sciences and Engineering Research Council of Canada (NSERC) through the CREATE grant entitled "Program on Advanced Polymer Composite Materials and Technologies (No. 511011-2018), as well as through a Discovery Grant secured by the corresponding author. Zoltek Corporation is also acknowledged for providing the unidirectional non-crimp fabric that was studied. Finally, the authors thank Ulrich Förter-Barth, Cahit Arik, and Kevin Moritz from the Fraunhofer Institute for Chemical Technology, Karlsruhe who provided support in performing the experiments.

Appendix A. Supplementary material

Supplementary data to this article can be found online at https://doi.org/10.1016/j.compositesa.2025.109347.

Data availability

The normalized moment-curvature data is available through supplementary material (spreadsheet).

References

[1] Ermanni P, Di Fratta C, Trochu F. Molding: Liquid Composite Molding. In: *Wiley Encyclopedia of Composites*. Wiley; 2012. p. 1–10. https://doi.org/10.1002/9781118097298.weoc153.
[2] Viisainen JV, Hosseini A, Sutcliffe MPF. Experimental investigation, using 3D digital image correlation, into the effect of component geometry on the wrinkling behaviour and the wrinkling mechanisms of a biaxial NCF during preforming. Compos A Appl Sci Manuf 2021;142:106248. https://doi.org/10.1016/j.compositesa.2020.106248.
[3] Beardmore P, Johnson CF. The potential for composites in structural automotive applications. Compos Sci Technol 1986;26(4):251–81. https://doi.org/10.1016/0266-3538(86)90002-3.
[4] F. Henning, L. Kärger, D. Dörr, F. J. Schirmaier, J. Seuffert, and A. Bernath, "Fast processing and continuous simulation of automotive structural composite components," Feb. 08, 2019, *Elsevier Ltd*. doi: 10.1016/j.compscitech.2018.12.007.
[5] Kruckenberg TM, Paton R, editors. *Resin Transfer Moulding for Aerospace Structures*. Dordrecht: Springer Netherlands; 1998. https://doi.org/10.1007/978-94-011-4437-7.
[6] H. Yang, C.-C. Hsu, and C.-H. Hsu, "Three dimensional numerical simulations for Wet-RTM process," in *35th Polymer Processing Society*, Cesme-Izmir, Turkey, 2019.
[7] J. Fels, G. Meirson, V. Ugresic, P. Dugsin, F. Henning, and A. Hrymak, "Mechanical property difference between composites produced using vacuum-assisted liquid compression molding and high-pressure injection resin transfer molding," in *Proceedings ACCE2017-17th Annual Automotive Composites Conference and Exhibition, Michigan*, 2017.
[8] Ghazimoradi M, Trejo EA, Carvelli V, Butcher C, Montesano J. Deformation characteristics and formability of a tricot-stitched carbon fiber unidirectional non-crimp fabric. Compos A Appl Sci Manuf 2021;145:106366. https://doi.org/10.1016/J.COMPOSITESA.2021.106366.
[9] S. V. Lomov, *Non-crimp fabric composites*. Cambridge, UK: Woodhead Publishing Limited, 2011. doi: 10.1533/9780857092533.
[10] L. Kärger, S. Galkin, E. Kunze, M. Gude, and B. Schäfer, "Prediction of forming effects in UD-NCF by macroscopic forming simulation–Capabilities and limitations," in *ESAFORM 2021 - 24th International Conference on Material Forming*, Liège, Belgium, 2021.
[11] Boisse P, Hamila N, Guzman-Maldonado E, Madeo A, Hivet G, Dell'Isola F. The bias-extension test for the analysis of in-plane shear properties of textile composite reinforcements and prepregs: a review. Int J Mater Forming 2017;10:473–92.
[12] C. D. Rudd, A. C. Long, K. N. Kendall, and C. G. E. Mangin, "Liquid moulding technologies," 1997.
[13] Kumar R, Rashvand K, Fraisse A, Sarhadi A, Andersen TL. Experimental testing method to characterise the drapability of UD non-crimp fabrics used in wind turbine blades. IOP Conf Ser: Mater Sci Eng 2023;1293(1):012020. https://doi.org/10.1088/1757-899x/1293/1/012020.
[14] Estrada G, Vieux-Pernon C, Advani SG. Experimental characterization of the influence of tackifier material on preform permeability. J Compos Mater 2002;36(19):2297–310. https://doi.org/10.1177/0021998302036019542.
[15] Brody JC, Gillespie JW. The effects of a thermoplastic polyester preform binder on vinyl ester resin. J Thermoplast Compos Mater 2005;18(3):157–79. https://doi.org/10.1177/0892705705043535.
[16] Yoo HM, Lee JW, Kim JS, Um MK. Influence of non-reactive epoxy binder on the permeability and friction coefficient of twill-woven carbon fabric in the liquid composite molding process. Appl Sci (Switzerland) 2020;10(20):1–13. https://doi.org/10.3390/app10207039.
[17] Neunkirchen S, Bender M, Schledjewski R. Effect of binder activation on in-plane capillary flow in multilayer stacks of carbon fiber fabrics. Appl Compos Mater 2024;31(2):709–19. https://doi.org/10.1007/s10443-023-10198-6.
[18] Wei K, Liang D, Mei M, Wang D, Yang X, Qu Z. Preforming behaviors of carbon fiber fabrics with different contents of binder and under various process parameters. Compos B Eng 2019;166:221–32. https://doi.org/10.1016/j.compositesb.2018.11.143.
[19] R. M. Portela, B. Schäfer, L. Kärger, A. Rocha De Faria, and J. Montesano, "Influence of Viscosity, Binder Activation, and Loading Rate on the Membrane Response of an Infiltrated UD-NCF," in *ESAFORM 2024 - 27th International Conference on Material Forming*, Toulouse, Apr. 2024.
[20] P. H. Broberg, F. Shakibapour, J. Jakobsen, E. Lindgaard, and B. L. V Bak, "Characterisation of the transverse shear behaviour of binder-stabilised preforms for wind turbine blade manufacturing," 2023, doi: 10.17632/9m78sg3zwn.1.
[21] Poppe C. Process simulation of wet compression moulding for continuous fibre-reinforced polymers. Karlsruhe: Karlsruhe Institute of Technology; 2021. Doctoral Thesis.
[22] J. Pourtier, B. Duchamp, M. Kowalski, X. Legrand, P. Wang, and D. Soulat, "Bias extension test on a bi-axial non-crimp fabric powdered with a non-reactive binder system," in *ESAFORM 2018 - 21st International Conference on Material Forming*, Palermo, Italy, 2018.
[23] de Bilbao E, Soulat D, Hivet G, Gasser A. Experimental study of bending behaviour of reinforcements. Exp Mech 2010;50(3):333–51. https://doi.org/10.1007/s11340-009-9234-9.
[24] Martin TA, Bhattacharyya D, Collins IF. Bending of fibre-reinforced thermoplastic sheets. Compos Manuf 1995;6(3):177–87. https://doi.org/10.1016/0956-7143(95)95009-N.
[25] Boisse P. Composite Fiber Reinforcement Forming. In: Wiley Encyclopedia of Composites. Wiley; 2011. p. 1–16. https://doi.org/10.1002/9781118097298.weoc037.
[26] Boisse P, Colmars J, Hamila N, Naouar N, Steer Q. Bending and wrinkling of composite fiber preforms and prepregs. A review and new developments in the draping simulations. Compos B Eng 2018;141:234–49. https://doi.org/10.1016/J.COMPOSITESB.2017.12.061.
[27] Yu WR, Zampaloni M, Pourboghrat F, Chung K, Kang TJ. Analysis of flexible bending behavior of woven preform using non-orthogonal constitutive equation. Compos A Appl Sci Manuf 2005;36(6):839–50. https://doi.org/10.1016/j.compositesa.2004.10.026.
[28] Sachs U, Akkerman R. Viscoelastic bending model for continuous fiber-reinforced thermoplastic composites in melt. Compos A Appl Sci Manuf 2017;100:333–41. https://doi.org/10.1016/J.COMPOSITESA.2017.05.032.
[29] Sourki R, Khatir B, Najar SS, Vaziri R, Milani AS. Characterization of the dissipative large deformation bending response of dry fabric composites as occurs during forming. Compos Struct 2023;310:116728.
[30] Senner T, Kreissl S, Merklein M, Meinhardt M, Lipp A. Bending of unidirectional non-crimp-fabrics: experimental characterization, constitutive modeling and application in finite element simulation. Prod Eng 2015;9:1–10.
[31] Krogh C, Broberg PH, Kepler J, Jakobsen J. Comprehending the bending: a comparison of different test setups for measuring the out-of-plane flexural rigidity of a UD fabric. Key Eng Mater 2022;926:1257–67.
[32] Poppe C, Rosenkranz T, Dörr D, Kärger L. Comparative experimental and numerical analysis of bending behaviour of dry and low viscous infiltrated woven fabrics. Compos A Appl Sci Manuf 2019;124:105466. https://doi.org/10.1016/J.COMPOSITESA.2019.05.034.
[33] Peirce FTTI. The 'handle' of cloth as a measurable quantity. J Textile Inst Trans 1930. https://doi.org/10.1080/19447023008661529.
[34] Liang B, Chaudet P, Boisse P. Curvature determination in the bending test of continuous fibre reinforcements. Strain 2017;53(1):1–12. https://doi.org/10.1111/str.12213.
[35] Liang B, Hamila N, Peillon M, Boisse P. Analysis of thermoplastic prepreg bending stiffness during manufacturing and of its influence on wrinkling simulations. Compos A Appl Sci Manuf 2014;67:111–22. https://doi.org/10.1016/j.compositesa.2014.08.020.
[36] Clapp TG, Peng H, Ghosh TK, Eischen JW. Indirect measurement of the moment-curvature relationship for fabrics. Text Res J 1990;60(9):525–33. https://doi.org/10.1177/004051759006000906.
[37] Broberg PH, et al. One-click bending stiffness: Robust and reliable automatic calculation of moment-curvature relation in a cantilever bending test. Compos B Eng 2023;260:110763. https://doi.org/10.5281/zenodo.7376939.
[38] Broberg PH, et al. That's how the preform crumples: Wrinkle creation during forming of thick binder-stabilised stacks of non-crimp fabrics. Compos B Eng 2024;273. https://doi.org/10.1016/j.compositesb.2024.111269.

[39] Broberg PH, Lindgaard E, Thompson AJ, Belnoue J-P-H, Hallett SR, Bak BLV. An accurate forming model for capturing the nonlinear material behaviour of multilayered binder-stabilised fabrics and predicting fibre wrinkling. Compos B Eng 2024;274:111268. https://doi.org/10.1016/j.compositesb.2024.111268.
[40] Ghazimoradi M, Trejo EA, Butcher C, Montesano J. Characterizing the macroscopic response and local deformation mechanisms of a unidirectional non-crimp fabric. Compos A Appl Sci Manuf 2022;156:106857. https://doi.org/10.1016/j.compositesa.2022.106857.
[41] Ghazimoradi M, Montesano J. Macroscopic forming simulation for a unidirectional non-crimp fabric using an anisotropic hyperelastic material model. Appl Compos Mater 2023;30(6):2001–23. https://doi.org/10.1007/s10443-023-10158-0.
[42] Rouf K, Worswick MJ, Montesano J. A multiscale framework for predicting the mechanical properties of unidirectional non-crimp fabric composites with manufacturing induced defects. J Compos Mater 2021;55(6):741–57. https://doi.org/10.1177/0021998320958189.
[43] Lomov SV, Verpoest I, Peeters T, Roose D, Zako M. Nesting in textile laminates: geometrical modelling of the laminate. Compos Sci Technol 2003;63(7):993–1007. https://doi.org/10.1016/S0266-3538(02)00318-4.
[44] Heß H, Himmel N. Structurally stitched NCF CFRP laminates. Part 1: experimental characterization of in-plane and out-of-plane properties. Compos Sci Technol 2011;71(5):549–68. https://doi.org/10.1016/j.compscitech.2010.11.012.
[45] J. Wang, H. Lin, A. C. Long, M. J. Clifford, and P. Harrison, "Predictive modelling and experimental measurement of the bending behaviour of viscous textile composites," in *International ESAFORM Conference on Materials Forming*, Glasgow, U.K., 2006.
[46] Abbott GM, Grosberg P. The fabric cantilever. Text Res J 1966;36(10):930–2. https://doi.org/10.1177/004051756603601013.
[47] Grosberg P. The mechanical properties of woven fabrics part II: the bending of woven fabrics. Text Res J 1966;36(3):205–11. https://doi.org/10.1177/004051756603600301.
[48] Lahey TJ, Heppler GR. Mechanical modeling of fabrics in bending. J Appl Mech 2004;71(1):32–40. https://doi.org/10.1115/1.1629757.
[49] Haanappel SP, Ten Thije RHW, Sachs U, Rietman B, Akkerman R. Formability analyses of uni-directional and textile reinforced thermoplastics. Compos A Appl Sci Manuf 2014;56:80–92. https://doi.org/10.1016/j.compositesa.2013.09.009.